

<https://doi.org/10.1038/s41529-024-00501-6>

UV LED ageing of polymers for PV cell encapsulation

Nicolas Pinochet¹, Lucie Pirot-Berson¹, Romain Couderc¹ ✉ & Sandrine Therias²

Encapsulation polymers in terrestrial solar modules degrade due to ultraviolet radiation from the sun. To assess a polymer's durability under UV light, accelerated aging tests can be conducted. A new LEDs device allows us to investigate the effects of temperature, irradiation, and UV source spectrum on the photooxidation mechanism and kinetics of two polyethylene-based commercial encapsulants, differentiated by the presence or absence of UV absorbers. The photooxidation rate of the polymer matrix increases as the temperature and irradiance increase between 62 and 82 °C, and 12 and 28 W.m⁻², respectively. In the last case, the photooxidation rate is not proportional to the number of photons. Finally, we observed different distributions of degradation products under UVB radiation at 305 nm compared to those under UVA radiation at 365 nm. UVB photons enable Norrish reactions that are not possible with UVA alone. Special care is needed to maintain a balance between UVA and UVB photons to ensure representative durability tests. With a few adjustments to their emission spectrum, UV LED devices appear to be good candidates for accelerated aging of encapsulation polymers.

Photovoltaic (PV) silicon-based cells have been used as a clean energy source since the 1970s. To date, their efficiency has been improving continuously thanks to advances in architecture, materials, and processing¹. To preserve their high performance against environmental stresses such as mechanical load, corrosive chemicals, temperature, and high-energy light, they rely on the PV module structure to minimize the induced degradation mechanisms. PV modules are generally made of front and back protection layers that surround two polymer sheets that encapsulate PV cells. The front layer is usually made of glass, and the back layer can be glass or a multilayer polymer (backsheet). The polymer sheets inside the module are called encapsulants. They are key players in light transmission, electrical insulation, mechanical stress absorption, heat removal, chemical barrier protection and PV module integrity. To maintain such properties throughout a module lifetime that is now ~30 years², encapsulants must cope with the most stringent terrestrial conditions that lead to highly detrimental chemical reactions such as hydrolysis or photooxidation. Concerning terrestrial applications, most photodegradation reactions of encapsulants involve UV light between 300 and 400 nm³. Consequently, accelerated photoaging tests are usually run under various UV sources, including xenon arcs or fluorescent tubes, which simulate this part of the solar spectrum⁴.

Most current encapsulation polymers are made by copolymerizing ethylene with another species that does not absorb solar UV light that is received on the Earth's surface; these materials include vinyl acetate or acrylic acid⁵, leading to polymers containing polyethylene sequences such as poly(ethylene vinyl acetate) (EVA). Therefore, in a standard atmosphere,

the encapsulation polymer will undergo polyethylene-like photodegradation, which is more likely to occur via photooxidation⁶. This chain reaction mechanism is initiated by the absorption of a UV photon by a chromophore impurity, leading to a radical species capable of hydrogen abstraction from the polymer matrix. The formation of other radicals through successive hydrogen abstraction will propagate across the material, eventually destroying it⁷. Photooxidation is mainly affected by the oxygen concentration, temperature, UV light wavelength, and irradiance^{8,9}. It is thus necessary to assess the actual influence of these materials in the context of PV cell encapsulation to design fast and reliable accelerated photoaging tests that can reveal the severity of natural degradation in the long run. The ageing of certain classic polymers such as polyethylene has been studied under different environmental conditions. S. Therias et al. and A. Fairbrother et al. investigated the effects of temperature and UV irradiance on the photooxidation kinetics of low- and high-density polyethylenes, respectively¹⁰⁻¹². They found that both polyethylenes were degraded faster at higher temperatures in the 30–65 °C range. However, the acceleration of polyethylene aging through increased UV irradiance was possible up to ~50 W.m⁻². Above this threshold, the photooxidation rate remained constant. The effect of temperature and irradiance on photooxidation kinetics may sometimes be modeled using empirical or semiempirical laws as a mean to extrapolate aging kinetics to different environmental conditions and longer aging duration. Among the most widely used laws, Arrhenius's law correlates temperature with the rate constant of a chemical reaction¹³, and the law of reciprocity links the photoreaction rate to irradiance¹⁴. Regarding the effect

¹University of Grenoble Alpes, CEA, LITEN, DTS, INES, F-38000, Grenoble, France. ²Université Clermont Auvergne-CNRS, ICCF, Clermont-Ferrand, France.

✉ e-mail: romain.couderc@cea.fr

of UV source spectrum, J.-F. Glikman et al. studied the impact of irradiation wavelength on the photooxidation mechanism of EVA copolymers under short (254 nm) and long wavelengths (>300 nm)¹⁵. They highlighted the importance of selecting wavelengths near 300 nm for tests that address terrestrial photoaging, in order to avoid reactions such as acetate photolysis that may occur at shorter wavelength but not under sunlight. After comparing the behavior of different polymers for PV cell encapsulation under fluorescent tubes or a filtered xenon arc lamp, Heidrich et al. recommended using a lamp whose UV spectrum is similar to that of the solar spectrum for encapsulant aging tests¹⁶. However, UV LED technology, with its adjustable thin spectrum, is now mature enough to be applied to polymer aging tests¹⁷.

In this paper, we investigate the effects of aging conditions modification on the photooxidation mechanism and kinetics of commercial encapsulants in newly developed UV LED devices emitting at different wavelengths. To this end, we studied the behavior of two thermoplastic polyolefins (TPOs) designed for encapsulation of PV cells under photooxidative conditions with varying temperatures, UV irradiance, and emission spectrum.

Results and discussion

Influence of temperature

This study examined how temperature affects the photooxidation of a polymer matrix in encapsulants. TPO1 thin films were exposed to 20 W.m⁻² UV light in the 305 nm LEDs chamber at four temperatures: 62, 68, 74, and 82 °C. Figure 1 displays the changes in the IR absorption spectra of TPO1 films that were subjected to 600 h of irradiation. All the films irradiated at 305 nm and 82 °C broke after 400 h due to advanced photooxidation.

For all four temperatures, the IR spectra indicate the systematic emergence of absorption bands in the carbonyl domain linked to the photooxidation of the polymer matrix. The corresponding species are listed in Table 1.

Figure 1 shows that the higher the temperature is, the greater the absorbance for a given aging time. This means that photooxidation of the polymer matrix is accelerated by temperature increases between 62 and 82 °C.

This temperature dependency can be described by an Arrhenius behavior law to determine the apparent activation energy for photooxidation, E_a . Figure 2 shows the increase in the absorbance of the IR band

corresponding to carboxylic acids (1712 cm⁻¹), which was selected for its well-defined absorption maximum, as a function of irradiation time at different temperatures. The error bars represent the standard deviation of the absorbance of the sample triplicates.

Each curve in Fig. 2 can be divided into two parts. The first part is the induction period and covers the time between the beginning of the test and the point at which photooxidation products are detected by IR spectroscopy. This induction time is ~100 h for samples aged at 82 °C, which is twice as long as that for other temperatures.

In Fig. 2, between 400 and 600 h, we extracted the speeds v (in h⁻¹) at the different temperatures by determining the slope of the linear regression of these portions of the curves. E_a may then be determined from the following equation derived from the Arrhenius law:

$$\ln \frac{v}{v_0} = \frac{-E_a}{RT} + \ln a \quad (1)$$

with $v_0 = 1 \text{ h}^{-1}$, R the perfect gas constant, T the temperature (in K), and a variable depending on the concentration of the chemical species involved in the photooxidation process.

Figure 3 displays the evolution of the natural logarithm of v/v_0 as a function of the inverse of the temperature.

The data relating to the measurements taken at 82 °C have no associated error bar, as only a single film did not rupture before 600 h. The obtained curve can be fitted to a straight red line with an interpolation coefficient R^2 of 0.988. This finding implies that the photooxidation kinetics of the polymer matrix may follow an Arrhenius law. Consequently, an E_a of 160 kJ.mol⁻¹ is obtained from the red line in Fig. 3. However, UV absorbers may also degrade under UV light¹⁸ depending on the temperature and impact the E_a calculation because UV absorbers influence the photooxidation rate of the polymer matrix. Changes in the concentration of UV absorbers in the TPO1 films under these aging conditions were investigated via UV-visible spectroscopy to test this hypothesis. Figure 4 depicts the time- and temperature-dependent variations in the absorbance at 332 nm of the TPO1 films, which are attributable to the UV absorbers.

Figure 4 shows a continuous decrease in the absorbance at 332 nm for all temperatures and, consequently, for the corresponding concentrations of the UV absorbers in the TPO1 thin films. The UV absorber content in the

Fig. 1 | IR spectra of TPO1 films during irradiation with 305 nm UV LEDs at 20 W.m⁻² and different temperatures. a 62, b 68, c 74, and d 82 °C. The color gradient (purple to yellow) for the curves in each panel indicates the irradiation time undergone prior to measurement from 0 to 250 h in steps of 25 h and from 250 to 600 h in steps of 50 h.

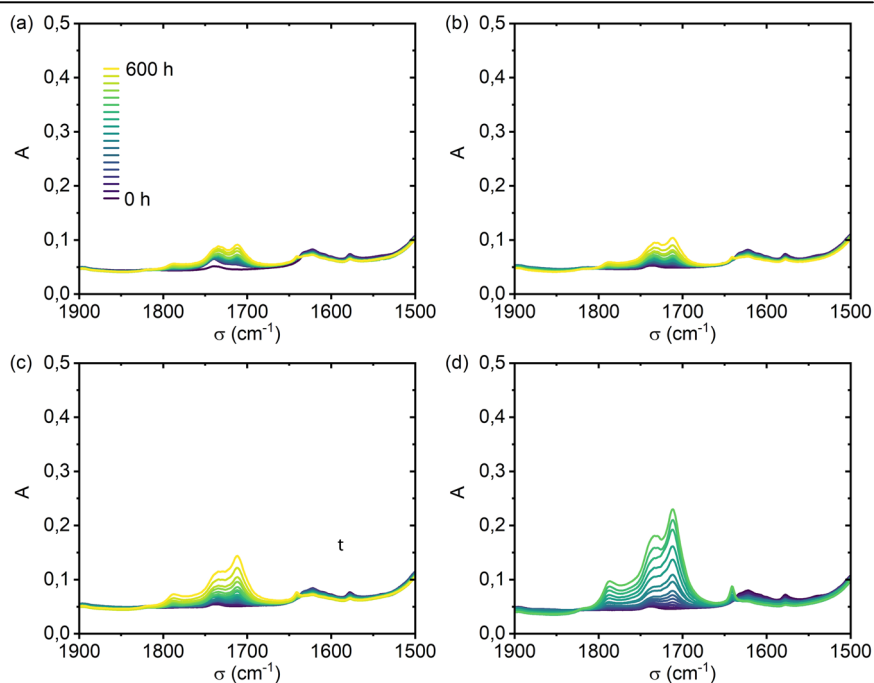
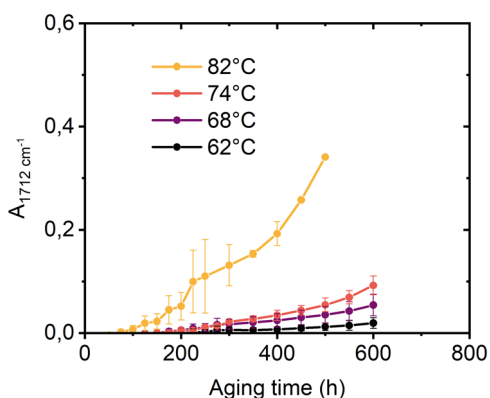
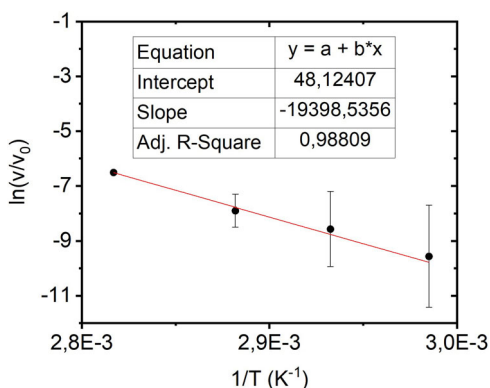


Table 1 | IR absorption maxima of carbonyl species formed during TPO1 photooxidation⁷

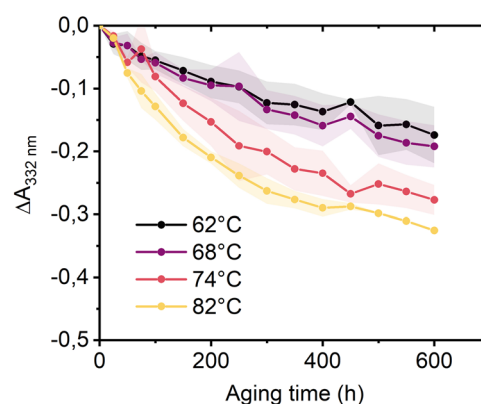
Wavenumber (cm ⁻¹)	Product
1780	Lactone
1735	Ester
1720	Ketone
1712	Carboxylic acid

**Fig. 2 |** Absorbance at 1712 cm⁻¹ (related to carboxylic acids) during TPO1 film photoaging under 305 nm LEDs at various temperatures (62, 68, 74, and 82 °C).**Fig. 3 |** Determination of E_a for TPO1 (films irradiated with 305 nm LEDs at 20 W.m⁻²) using the Arrhenius method.

films evolves differently according to the aging temperature. Because UV absorbers reduce the rate of photooxidation in the polymer matrix, such discrepancies in the disappearance rates impact TPO1 photooxidation kinetics and can also explain the important uncertainties in E_a .

To overcome the effect of UV absorbers, we analyzed the photooxidation kinetics of TPO2, which shares an identical polymer matrix with TPO1 but lacks UV absorbers. Thin films of TPO2 were exposed to 305 nm LEDs with the same irradiance (20 W.m⁻²) and temperature conditions (62, 68, 74 and 82 °C) as those used for TPO1. Tests were run up to 700 h. The samples were then analyzed using transmission FTIR spectroscopy. Figure 5 displays the evolution of the IR absorption spectra during photoaging.

Figure 5 shows that the increase in the carbonyl band density with temperature was quicker for TPO2 than for TPO1. For the same period of testing, the IR spectra of the TPO2 films showed noticeably greater absorbance levels than did those of the TPO1 films. This could be attributed to the delayed photooxidation of the TPO1 polymer matrix due to the UV absorption. As displayed in Fig. 1 for TPO1, Fig. 5 demonstrates that the

**Fig. 4 |** Changes in the absorbance at 332 nm of TPO1 films during UV aging with 305 nm LEDs at various temperatures (62, 68, 74, and 82 °C). The colored bands indicate measurement uncertainties.

absorbance ratios at 1712 and 1730 cm⁻¹ imply that a higher aging temperature marginally favors the production of carboxylic acid (1712 cm⁻¹) over ester (1730 cm⁻¹) during the photooxidation of TPO2 films. This change was not observed in the TPO1 IR spectra due to a lesser photooxidation progress.

To determine the E_a for the TPO2 films, the changes in the IR absorbance at 1712 cm⁻¹ are plotted as a function of aging time in Fig. 6.

By conducting a linear regression analysis of the linear region between 500 and 700 h, we can establish the apparent reaction rate, v . Figure 7 displays the natural logarithm plot of the ratio of these constants to the unit rate, v_0 , against the inverse of temperature.

Linear regression of the curve yields an interpolation coefficient R^2 of 0.997, indicating that the observed degradation mechanism follows an Arrhenius law. The determined E_a for the TPO2 films was 140 ± 10 kJ.mol⁻¹, which is within the range of E_a values previously reported in the literature for polyethylene photooxidation (60¹⁹ to 160 kJ.mol⁻¹²⁰). We have previously studied the photooxidation of LDPE at long wavelengths ($\lambda > 300$ nm and UV irradiances at 90 or 300 W.m⁻²) and obtained an E_a of 100–110 kJ.mol⁻¹¹⁰. The temperature and sample dependency of the rate at which UV absorbers disappear, which affects TPO1 photooxidation kinetics, may explain the 10-fold lower uncertainty in the E_a obtained for TPO2. Furthermore, the aim of the study is to give the reader insights into the choice of test conditions for concurrent aging acceleration and representative degradation of encapsulation polymers. The values obtained (e.g., activation energies) relate only to the encapsulants studied as an example, and cannot be extrapolated to these same polymers under different irradiation conditions (e.g., under glass), nor to polymers with different formulations.

Influence of UV irradiance

To investigate the impact of different levels of UV irradiance on the mechanism and kinetics of encapsulant photooxidation, we irradiated thin TPO1 films for 500 h at varying irradiances under 305 nm LEDs at 82 °C: 12, 20, and 28 W.m⁻². For each set of conditions, three samples were subjected to UV-visible and FTIR transmission spectroscopy analyses to monitor both the disappearance of the UV absorbers and polymer oxidation. Measurements after 450 and 500 h were not possible for some samples irradiated at 20 and 28 W.m⁻² due to significant tearing of the films.

UV-visible spectroscopy was performed to investigate the impact of irradiance on UV absorber deterioration under UV radiation. Figure 8 shows the variation in absorbance at 332 nm ($\Delta A_{332 \text{ nm}}$) for TPO1 films exposed to 305 nm UV light at 82 °C and varying irradiance.

The graphs for the varying UV irradiances are superimposed in Fig. 8, indicating that the kinetics of disappearance of the UV absorbers for the TPO1 thin films do not depend on irradiance. Consequently, the variation in the photooxidation rate of the polymer matrix between 12 and 28 W.m⁻²

Fig. 5 | IR spectra of TPO2 films under 305 nm LEDs irradiation at 20 W.m⁻² and different temperatures. a 62, (b) 68, (c) 74 and (d) 82 °C. The color gradient (purple to yellow) for the curves in each panel indicates the irradiation time undergone prior to measurement from 0 to 700 h in steps of 100 h.

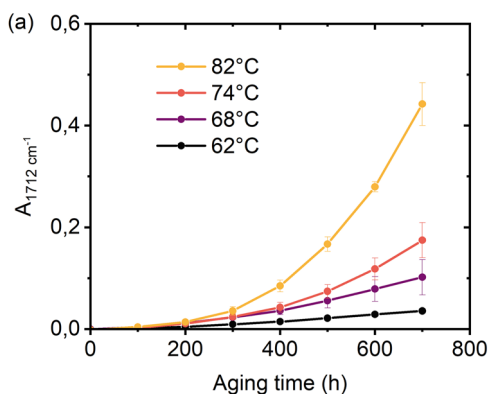
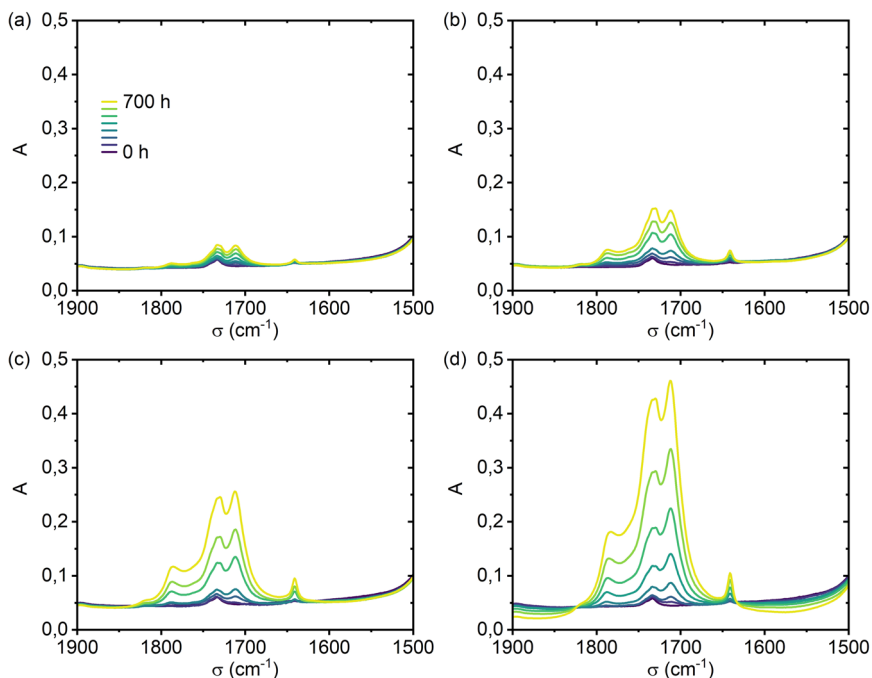


Fig. 6 | Absorbance at 1712 cm⁻¹ (related to carboxylic acids) during TPO2 film photoaging under 305 nm LEDs at various temperatures (62, 68, 74, and 82 °C).

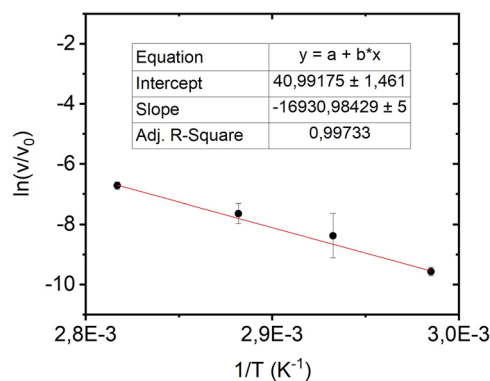


Fig. 7 | Determination of Ea for TPO2 (films irradiated under 305 nm LEDs at 20 W.m⁻²) using the Arrhenius method.

is not affected by the disappearance of the UV absorbers. Because of the thinness of the films and its temperature dependence, the depletion of UV absorbers may then be explained by diffusion processes coupled to evaporation from the film surface. While UV absorbers are consumed in a PV module exposed to UV light through a yellowing-photobleaching mechanism²¹ and diffusion of such additives through encapsulant is possible²², the limited interface between air and encapsulant may prevent UV absorbers evaporation. As such, the photooxidation resistance of several encapsulation polymers protected by UV absorbers must be compared considering the loss of UV absorbers by diffusion-evaporation in the case of thin films. Using thick samples and comparing their core state after aging tests may be an alternative solution.

Because no discrepancy was observed in the UV absorber depletion under the different irradiances, as shown in Fig. 8, the samples were subjected to FTIR measurements. Figure 9 shows the IR spectra of TPO1 films exposed to 305 nm UV light at 82 °C and varying irradiance.

The intensity of the carbonyl absorption bands increased with age under the three irradiances. Figure 9 shows that faster photooxidation of TPO1 films occurs at higher irradiance levels in the range of 12–28 W.m⁻². At the same level of progress (for example, with the same

level of absorbance at 1712 cm⁻¹), the ratios of the various oxidation products do not seem to change with irradiance. Hence, the evolution of A_{1712 cm⁻¹} is still considered a good indicator of photooxidation. The IR absorbance at 1712 cm⁻¹ for TPO1 films aged at different irradiances is plotted in Fig. 10.

The plots in Fig. 10 exhibit an initial induction period of 100 h, followed by the spread of photooxidation within the thin films for at least 400 h. We investigated the accuracy of the law of reciprocity corrected with the Schwarzschild coefficient applied to the photooxidation kinetics of the TPO1 films:

$$[P] \propto t \times I^p \quad (2)$$

where $[P]$ is the concentration of stable photooxidation products at time t , I is the UV irradiance and p is the Schwarzschild coefficient.

Equation (3) is then derived from Eq. (2):

$$\log t = \log(bA) - p \log I \quad (3)$$

where b is a constant and A is the absorbance at time t .

In Fig. 10, $A_{1712\text{ cm}^{-1}} = 0.18$ corresponds to a data point obtained during the propagation of photooxidation under each irradiance. In Fig. 11, we plot the logarithm of the time required to achieve $A_{1712\text{ cm}^{-1}} = 0.18$ as a function of the logarithm of the normalized irradiance ratio I/I_0 . Here, I is expressed in $\text{W}\cdot\text{m}^{-2}$, and I_0 is $1\text{ W}\cdot\text{m}^{-2}$.

The linear fit based on the data permitted the evaluation of the p coefficient. The determined value of p is 0.4 ± 0.1 . It can vary depending on the formulation of the TPO encapsulant, as was shown in the case of polyethylene stabilized with HALS antioxidant¹¹. Given that p is less than 1, a deviation from the law of reciprocity is observed. This means that the acceleration provided by the use of higher irradiances is not proportional to the irradiance. In other words, if sample A is irradiated for time t at an irradiance of $2 \times I$ and sample B is irradiated for $2 \times t$ at I , the two samples will not reach the same oxidation state. The photooxidation of sample B will be further advanced. This sublinear dependence on irradiance has already been reported¹⁰ and can be particularly discerned in the case of pristine low-density polyethylene (without stabilizers) irradiated at 60°C under long wavelengths ($\lambda > 300\text{ nm}$) with mercury lamps between 1 and $41.5\text{ W}\cdot\text{m}^{-2}$.

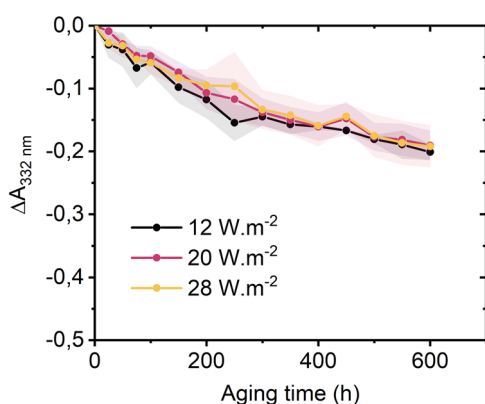
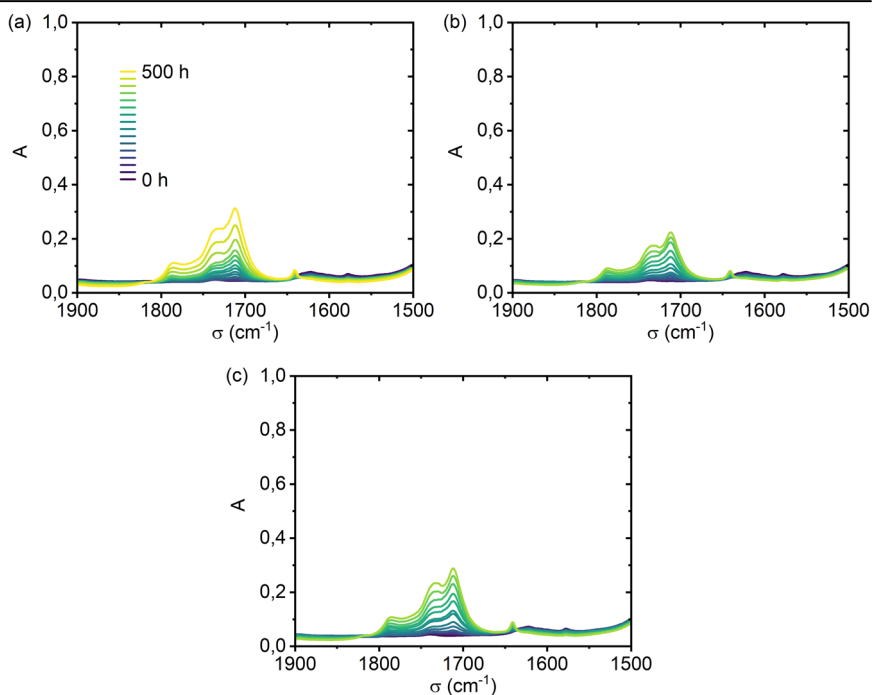


Fig. 8 | Variation in the absorbance at 332 nm of TPO1 during UV aging under 305 nm LEDs at 82°C and varying levels of irradiance (12, 20, and $28\text{ W}\cdot\text{m}^{-2}$). The colored bands indicate the measurement uncertainties.

Fig. 9 | IR spectra of TPO1 films during UV irradiation under 305 nm LEDs at 82°C and different irradiances. **a** 12, **b** 20 and **c** $28\text{ W}\cdot\text{m}^{-2}$. The color gradient (purple to yellow) for the curves in each panel indicates the irradiation time undergone prior to measurement from 0 to 300 h in steps of 25 h and from 300 to 500 h in steps of 50 h.



Influence of the UV source spectrum

We also investigated the influence of the emission spectrum of the UV lamp, i.e., the influence of the irradiation wavelength, on the photooxidation of the encapsulants by comparing the photooxidation mechanisms that occur in the two UV chambers. Individually, the UV LEDs devices cannot reproduce the real spectrum that modules will experience, but each can give us an understanding of the mechanisms caused by the thin range of wavelengths they emit. We irradiated thin films of TPO1 with 305 nm LEDs and 365 nm LEDs for 600 h. Photooxidation of the encapsulant was studied at 68°C with an irradiance of $28\text{ W}\cdot\text{m}^{-2}$ UVB (305 nm LEDs) and an irradiance of $980\text{ W}\cdot\text{m}^{-2}$ UVA (365 nm LEDs). In order to get comparable degradation severity (that is to say oxidation degree) for equal aging time between the two LEDs devices, we chose to set the irradiance to the maximum intensity for the 305 nm LEDs and the minimum intensity for the 365 nm LEDs. The differences in the emission spectra are shown in the methods section. Three films per exposure condition were characterized by FTIR spectroscopy. The IR absorption spectra measured during the tests are plotted in Fig. 12.

Figure 12a, b show the appearance of absorption bands corresponding to carbonyl groups formed during photooxidation of the polymer matrix in the TPO1 films. In both cases, the absorbance levels reached after 600 h are low due to the test temperature and the stabilization of the encapsulant by the UV absorbers. However, the polymer matrix was sufficiently oxidized to reveal differences in stoichiometry. The proportions of the different carbonylated products depend on the irradiation wavelength. In particular, the shoulder between the bands at 1730 cm^{-1} and 1712 cm^{-1} becomes very pronounced for the 365 nm LEDs whereas a dip is noticeable at 1720 cm^{-1} for the 305 nm LEDs. This difference may be due to the presence of ketones, which have an IR band at 1720 cm^{-1} . Such species are produced during photooxidation of the polymer matrix. However, ketones absorb at 320 nm and can be photochemically degraded by Norrish reactions into other species, such as carboxylic acids²³. As ketones absorb in the UVB range²⁴, they are consumed by irradiation with 305 nm LEDs but not with 365 nm LEDs. This phenomenon was described for polyethylene films in a recent paper of Bourgogne et al.¹⁷. The corresponding IR absorption band at 1720 cm^{-1} is therefore weaker under the 305 nm LEDs than under irradiation at 365 nm.

Thin films of TPO2 also underwent photoaging for 600 h under 305 nm LEDs and 365 nm LEDs at 68 °C. The films were analyzed through transmission FTIR spectroscopy, and the IR spectra are shown in Fig. 13.

Photooxidation of the polymer matrix is observed during aging under both UV lamps, as evidenced by the emergence of absorption bands for carbonyl products. However, photooxidation occurs at a notably slower rate under 365 nm LEDs. The sluggish oxidation rate after 600 h of irradiation with 365 nm LEDs could be explained by the low absorption at this wavelength of chromophore impurities present in the TPO2 films, in contrast to their absorption at 305 nm. The high photon absorption of UV absorbers under 305 nm LEDs could limit photooxidation more effectively than that at 365 nm. This could account for the slight variation in the photooxidation rate of TPO1 after 600 h under both 305 and 365 nm LEDs (see Fig. 12).

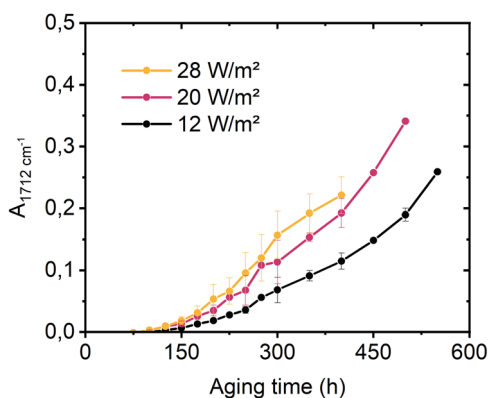


Fig. 10 | Absorbance at 1712 cm^{-1} (carboxylic acids) during aging of TPO1 at 82 °C and at different UV irradiances and at 12, 20, and 28 $\text{W}\cdot\text{m}^{-2}$ (305 nm LEDs).

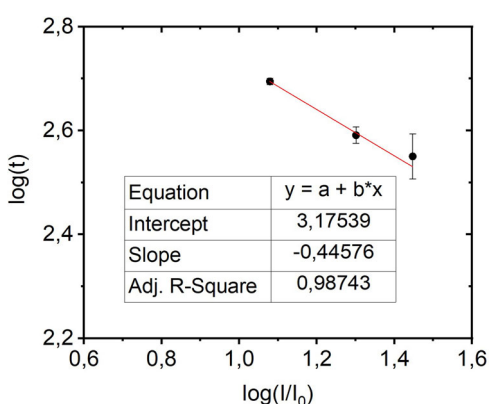
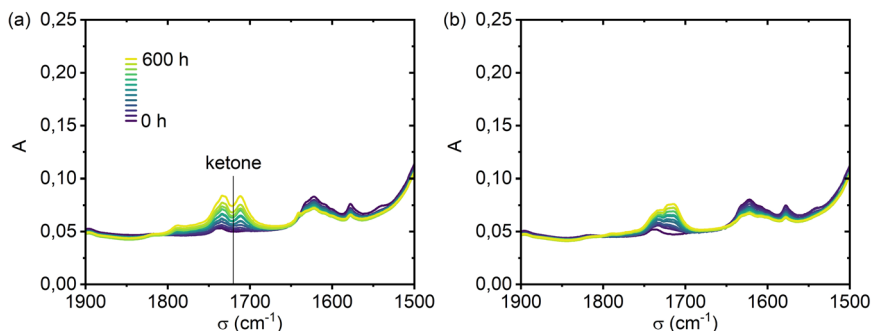


Fig. 11 | Determination of the Schwarzschild factor for TPO1 films irradiated with 305 nm LEDs at 82 °C.

Fig. 12 | IR images of TPO1 films irradiated at 68 °C under different UV LEDs. **a** 305 nm at 28 $\text{W}\cdot\text{m}^{-2}$, **b** 365 nm at 980 $\text{W}\cdot\text{m}^{-2}$. The color gradient (purple to yellow) for the curves in each panel indicates the irradiation time undergone prior to measurement from 0 to 600 h in steps of 50 h. A vertical black line indicates the position of ketones at 1720 cm^{-1} .



In summary, aging tests can be accelerated by elevating the temperature and UV irradiance but the emission spectrum of the UV source should be restricted to wavelengths above 300 nm. It is crucial to verify that the increase in temperature or irradiance does not impact photochemical mechanisms. Aging acceleration cannot always be modeled by simple laws such as the law of reciprocity without the Schwarzschild correction and requires investigations for a specific formulation. Moreover, aging test engineering should not allow additional mechanisms that impact the studied reactions and do not occur in the operating environment to occur in the test chamber. Thanks to their modularity in terms of temperature, irradiance and emission spectrum, LED devices can be used to study the effects of environmental stress variations on the aging of encapsulants, enabling research of test conditions for accelerated aging without distortion.

Methods

Two thermoplastic polyolefins (TPOs) (denoted as TPO1 and TPO2), which are polyethylene-based copolymers used for the encapsulation of solar cells, were studied. TPO1 and TPO2 share the same polymer matrix. According to the comparison of infrared TPO1 and polyethylene spectra in Fig. 14a, the composition of these encapsulants is similar to that of polyethylene. Although antioxidants and process additives might vary in nature and concentration between the TPOs formulation, TPO1, and TPO2 infrared spectra did not exhibit any significant difference that would allow additives identification. Nevertheless, TPO1 is a high-UV cutoff encapsulant that contains UV absorbers, while TPO2 does not. This difference can be observed in the UV-visible spectra, as shown in Fig. 14b.

The strong absorption between 300 nm and 360 nm with a maximum at 332 nm observed in the UV-visible spectrum of TPO1 can be attributed to the presence of UV absorbers. To carry out Fourier transform infrared (FTIR) spectroscopy analysis in transmission mode, pieces of industrial sheets were compressed under 200 bars and 160 °C for 5 min, from which $55 \pm 5 \mu\text{m}$ -thick films were cut. The pressing process might have an influence on the films morphology. Polymer morphology can affect the oxygen transport in the films and act indirectly on the photooxidation kinetics²⁵ but the photooxidation products will remain the same as in thicker films. In this study, we consider the worst case scenario when the oxygen ingress is maximum in the films. One can note that in a PV module different oxygen content in the film will result from the distance to the edge of the PV module and depending on the ability of oxygen to diffuse in the encapsulant.

The aging tests were run in two UWAVE LED UV chambers, referred to as 305 nm LEDs and 365 nm LEDs. In each chamber, the samples are irradiated by 25 LEDs that are arranged in a square formation. A sample holder designed according to a patented method provides different sample temperatures and irradiances during the same aging test²⁶. This device is heated by a heat plate, and the temperature is monitored by K-type thermocouples. The lamp spectra are shown in Fig. 15.

Three films of processed polymers were tested under each aging condition mentioned in Table 2.

FTIR measurements were performed with a Thermo Fisher Nicolet 5700 spectrometer (32 scans, 2 cm^{-1} resolution) between 4000 and 400 cm^{-1}

Fig. 13 | IR spectra of TPO2 films irradiated under different UV LEDs at 68 °C. a 305 nm at 28 W.m⁻², b 365 nm at 980 W.m⁻². The color gradient (purple to yellow) for the curves in each panel indicates the irradiation time undergone prior to measurement from 0 to 600 h in steps of 200 h.

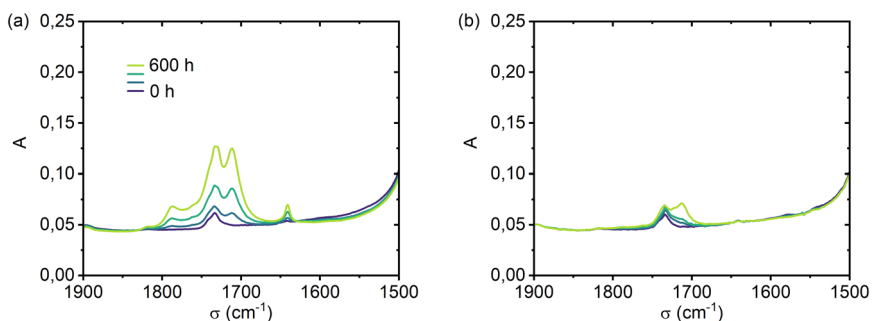


Fig. 14 | Comparison of polymers spectra. a FTIR spectra of polyethylene and TPO1 and TPO1 and (b) UV-visible spectra of TPO1 and TPO2.

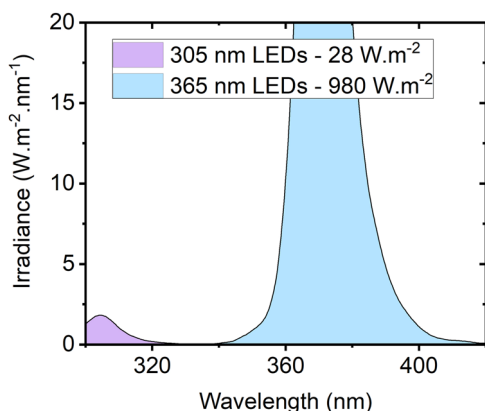
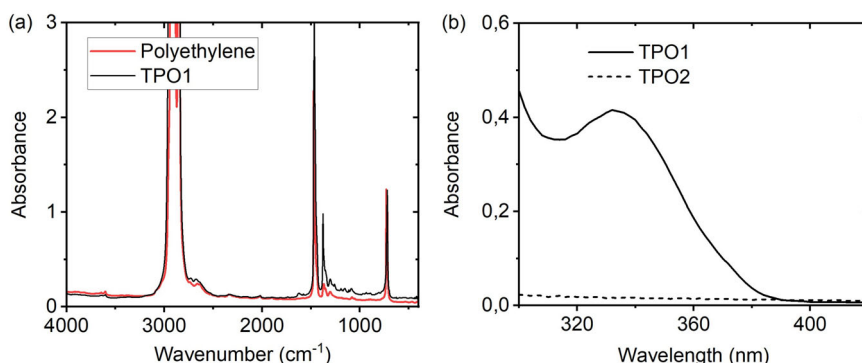


Fig. 15 | Emission spectra of UV sources.

Table 2 | UV aging test parameters

Analysis	UV chamber	UV irradiance (W.m ⁻²)	Sample temperature (°C)
Effect of temperature	UWAVE 305 nm LEDs	20	62
			68
			74
			82
Effect of irradiance	UWAVE 305 nm LEDs	12	82
		20	
		28	
Effect of emission spectrum	UWAVE 305 nm LEDs	28	68
	UWAVE 365 nm LEDs	980	

to detect carbonyl products from 1900 to 1500 cm⁻¹. A thickness correction was always applied to compensate for the small thickness discrepancies between films. Correction of thickness difference has been done by spectra homothety and superimposition of the absorption band at 720 cm⁻¹ (-CH₂ rocking) that does not vary with irradiation time. UV-visible spectroscopy was carried out with a Perkin Elmer Lambda 950 spectrometer (2 nm resolution) between 200 nm and 800 nm to monitor the stability of the UV absorbers between 280 and 450 nm.

Data availability

The relevant data are available from the corresponding author upon reasonable request.

Received: 25 February 2024; Accepted: 29 July 2024;
Published online: 14 August 2024

References

- National Renewable Energy Laboratory (NREL). Best research-cell efficiency chart. nrel.gov, 2021, [Online]. Available: <https://www.nrel.gov/pv/cell-efficiency.html>. Accessed 04 Aug 2021.
- Jean, J., Woodhouse, M. & Bulović, V. Accelerating photovoltaic market entry with module replacement. *Joule* **3**, 2824–2841 (2019).
- De Oliveira, M. C. C., Diniz, A. S. A. C., Viana, M. M. & Lins, VdeF. C. The causes and effects of degradation of encapsulant ethylene vinyl acetate copolymer (EVA) in crystalline silicon photovoltaic modules: a review. *Renew. Sustain. Energy Rev.* **81**, 2299–2317 (2018).
- Measurement procedures for materials used in photovoltaic modules-Part 7.2: Environmental exposures-Accelerated weathering tests of polymeric materials. IEC 62788-7-2 standard, 2017.
- Peike, C., Hädrivh, I., Weiß, K.-A. & Dürr, I. Overview of PV module encapsulation materials. *Photovolt. Int.* **19**, 85–92 (2013).
- Partridge, R. H. Near ultraviolet absorption spectrum of polyethylene. *J. Chem. Phys.* **45**, 1679–1684 (1966).
- Gardette, M. et al. Photo- and thermal oxidation of polyethylene: comparison of mechanisms and influence of unsaturation content. *Polym. Degrad. Stab.* **98**, 2383–2390 (2013).

8. Bigger, S. W., Scheirs, J. & Delatycki, O. Effect of light intensity on the photooxidation kinetics of high-density polyethylene. *J. Polym. Sci. Part A Polym. Chem.* **30**, 2277–2280 (1992).
9. Bigger, S. W. & Delatycki, O. Effects of temperature and the partial pressure of oxygen on the rate of photooxidation of polyethylene. *Polymer* **29**, 1277–1281 (1988).
10. Therias, S., Rapp, G., Masson, C. & Gardette, J.-L. Limits of UV-light acceleration on the photooxidation of low-density polyethylene. *Polym. Degrad. Stab.* **183**, 109443 (2021).
11. Mazeau, E. et al. Influence of irradiance on the photooxidation of HALS stabilized low-density polyethylene. *Polym. Degrad. Stab.* **216**, 110478 (2023).
12. Fairbrother, A. et al. Temperature and light intensity effects on photodegradation of high-density polyethylene. *Polym. Degrad. Stab.* **165**, 153–160 (2019).
13. Arrhenius, S. Über die Reaktionsgeschwindigkeit bei der Inversion von Rohrzucker durch Säuren. *Z. Phys. Chem.* **4U**, 226–248 (1889).
14. Martin, J. W., Chin, J. W. & Nguyen, T. Reciprocity law experiments in polymeric photodegradation: a critical review. *Prog. Org. Coat.* **47**, 292–311 (2003).
15. Glikman, J.-F., Arnaud, R., Lemaire, J. & Seneira, H. Photo-oxidation et photolyse de copolymères d'éthylène et d'acétate de vinyle à courte et grandes longueurs d'onde. *Die Makromol. Chem.* **188**, 987–1004 (1987).
16. Heidrich, R. et al. UV lamp spectral effects on the aging behavior of encapsulants for photovoltaic modules. *Sol. Energy Mater. Sol. Cells* **266**, 112674 (2024).
17. Bourgogne, D., Therias, S. & Gardette, J.-L. Wavelength effect on polymer photooxidation under LED weathering conditions. *Polym. Degrad. Stab.* **202**, 110021 (2022).
18. Pickett, J. E. Review and kinetics analysis of the photodegradation of UV absorbers. *Macromol. Symposia* **115**, 127–141 (1997).
19. Cruz-Pinto, J. J. C., Carvalho, M. E. S. & Ferreira, J. F. A. The kinetics and mechanism of polyethylene photo-oxidation. *Die Angew. Makromol. Chem.* **3872**, 133–133 (1994).
20. Corrales, T., Catalina, F., Peinado, C., Allen, N. S. & Fontan, E. Photooxidative and thermal degradation of polyethylenes: interrelationship by chemiluminescence, thermal gravimetric analysis and FTIR data. *J. Photochem. Photobiol. A: Chem.* **147**, 213–224 (2002).
21. Pinochet, N., Couderc, R. & Therias, S. Solar cell UV-induced degradation of module discolouration: between the devil and the deep yellow sea. *Prog. Photovolt. Res. Appl.* **31**, 1091–1100 (2023).
22. Heidrich, R., Lüdemann, M., Mordvinkin, A. & Gottschalg, R. Diffusion of UV additives in ethylene-vinyl acetate copolymer encapsulants and the impact on polymer reliability. *IEEE J. Photovolt.* **14**, 131–139 (2024).
23. Tidjani, A. Comparison of formation of oxidation products during photo-oxidation of linear low density polyethylene under different natural and accelerated weathering conditions. *Polym. Degrad. Stab.* **68**, 465–469 (2000).
24. Martinez, R. D., Buitrago, A. A., Howell, N. W., Hearn, C. H. & Joens, J. A. The near U.V. absorption spectra of several aliphatic aldehydes and ketones at 300 K. *Atmos. Environ. Part A. Gen. Top.* **26**, 785–792 (1992).
25. Vittoria, V. Influence of the crystallinity on the transport properties of polyethylene. *J. Mater. Sci.* **30**, 3954–3958 (1995).
26. Pinochet N., Couderc R., Therias S. Enceinte de photo-vieillessement à multi-irradiance. Patent FR2113280 (2021).

Author contributions

N.P., R.C., and S.T. conceived the study. N.P. performed samples preparation. N.P. and L.P.-B. performed experiments, data acquisition, and analysis under the supervision of R.C. and S.T. All authors discussed the data interpretation. N.P. wrote the paper's first draft, revised by all. All authors approved the final version.

Competing interests

The authors declare no competing interests.

Additional information

Correspondence and requests for materials should be addressed to Romain Couderc.

Reprints and permissions information is available at <http://www.nature.com/reprints>

Publisher's note Springer Nature remains neutral with regard to jurisdictional claims in published maps and institutional affiliations.

Open Access This article is licensed under a Creative Commons Attribution-NonCommercial-NoDerivatives 4.0 International License, which permits any non-commercial use, sharing, distribution and reproduction in any medium or format, as long as you give appropriate credit to the original author(s) and the source, provide a link to the Creative Commons licence, and indicate if you modified the licensed material. You do not have permission under this licence to share adapted material derived from this article or parts of it. The images or other third party material in this article are included in the article's Creative Commons licence, unless indicated otherwise in a credit line to the material. If material is not included in the article's Creative Commons licence and your intended use is not permitted by statutory regulation or exceeds the permitted use, you will need to obtain permission directly from the copyright holder. To view a copy of this licence, visit <http://creativecommons.org/licenses/by-nc-nd/4.0/>.

© The Author(s) 2024